

# Latitude gradient in aerosol properties across the Inter Tropical Convergence Zone: Results from the joint Indo-US study onboard *Sagar Kanya*

A. Jayaraman<sup>\*,§</sup>, S. K. Satheesh<sup>†</sup>, A. P. Mitra<sup>‡</sup> and V. Ramanathan<sup>†</sup>

<sup>\*</sup>Physical Research Laboratory, Navrangpura, Ahmedabad 380 009, India

<sup>†</sup>C4/CAS, Scripps Institution of Oceanography, UCSD, La Jolla, CA 92093-0221, USA

<sup>‡</sup>National Physical Laboratory, New Delhi 110 012, India

As part of the Indian Ocean Experiment (INDOEX) Intensive Field Phase (IFP), a cruise by ORV *Sagar Kanya* was conducted in the Arabian Sea and the Indian Ocean from 20 January to 12 March 1999. Measurements on aerosol properties such as optical depth, mass concentration, size distribution, scattering and absorption coefficients were measured using instruments such as sun-photometer, quartz crystal microbalance, nephelometer and particle-soot absorption photometer. One of the important findings is the large north-south asymmetry in the aerosol characteristics. Aerosol optical depth values were very high, exceeding 0.4, close to the west coast of India and the Arabian Sea, which is greater than by a factor of 4 or more, compared to the values south of the ITCZ. The wavelength exponent  $a$ , is found to be in the range of 1.3 to 1.7 in the high optical depth region and is in the range of 0.5 to 0.7 over the pristine region. Aerosol mass concentration data show that the nucleation mode aerosols (radius  $< 0.1 \mu\text{m}$ ) are systematically higher over the Arabian Sea, with values ranging from 20 to 50  $\mu\text{g}/\text{m}^3$ . Correlating the aerosol mass with the scattering coefficient, we get a scattering to mass concentration ratio of 2.27  $\text{m}^2/\text{g}$ , for the Arabian Sea region, which is in between the values reported by other workers, 3.3  $\text{m}^2/\text{g}$  for the continent and 1.67  $\text{m}^2/\text{g}$  for the marine regions, elsewhere in the world. The single scattering albedo,  $w$  derived from the scattering and absorption data, is around 0.9 for aerosols found over the Arabian Sea, while near the coastal regions the values are as low as 0.8. Low  $w$  and high optical depth found in the coastal region and Arabian Sea indicate large absorption by aerosols. The results undoubtedly show a large spatial difference in aerosol characteristics between north and south of the ITCZ which could lead to a large asymmetry in aerosol radiative forcing between the two regions.

CONTINENTS surrounding the Arabian Sea and the tropical Indian Ocean are responsible for the production of a variety of natural and anthropogenic aerosols. These aerosols

are transported over the ocean surface, to very long distances depending on the prevailing wind conditions, and can remain in the marine atmosphere for few days to few weeks, until lost into the ocean by gravitational settling or rain wash. Compared to well-mixed greenhouse gases, aerosols exhibit large spatial and temporal variations, and are responsible for producing large spatial inhomogeneity<sup>1</sup> in the surface reaching solar flux intensity. As the solar energy input to the ocean is one of the important factors which drive the earth's climate, study of the optical properties of aerosols and quantifying their radiative forcing form an important discipline in the climate change studies<sup>2</sup>. The prime objective of the Indian Ocean Experiment (INDOEX) is to delineate the natural and anthropogenic components in the aerosol radiative forcing and study its consequence on the regional and global climate change<sup>3</sup>. The INDOEX Intensive Field Phase (IFP) is the major international field effort conducted from January to April 1999 over the Indian Ocean region, across the Inter-Tropical Convergence Zone (ITCZ), where the polluted air from the continents meet the pristine air from the south.

## INDOEX-IFP cruise

The INDOEX-IFP cruise by ORV *Sagar Kanya* was conducted from 20 January to 12 March 1999 over the Arabian Sea and the tropical Indian Ocean from about 17°N to 20°S and 58° to 77°E. Figure 1 shows the cruise track. Values of some of the parameters measured along the cruise track are shown at a few selected locations. They are the date, wind direction, aerosol optical depth at 399 nm, aerosol optical depth at 1051 nm and the single scattering albedo respectively. These results are described in the later sections. The first transect, made during 20 January to 5 February was in the north south direction from 15°N to 20°S along the 73° to 77°E longitude belt. The data collected during the first transect included the coastal Indian region and open ocean regions north and south of the ITCZ. The observed wind during this period was generally from the northwest and northeast directions,

<sup>§</sup>For correspondence. (e-mail: jraman@prl.res.in)

bringing the continent air over the ocean till about 5°S. Below about 10°S the observed wind was predominantly from the east and southeast directions, which brought the pristine air from the south. The region between 5° and 10°S could be considered as the ITCZ region in the first transect. The second transect was in the east to west direction along the 20°S latitude from 77° to about 58°E, near Mauritius. The entire second transect, from 5 to 11 February, was south of the ITCZ, in the pristine region. However, the easterly wind (stern wind with respect to the

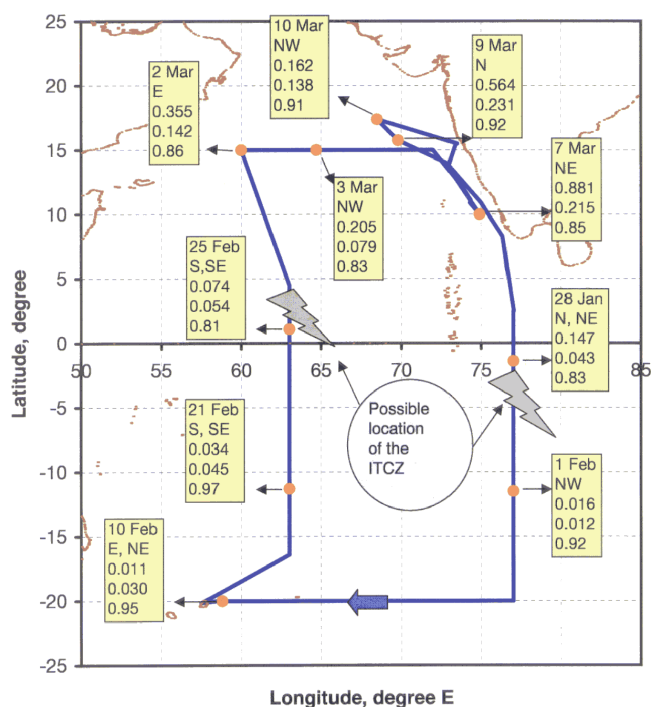


**Figure 1.** The ORV *Sagar Kanya* cruise track from 20 January to 11 March 1999 for the INDOEX-IFP experiments. At typical locations date of visit, wind direction, aerosol optical depth at 399 nm, aerosol optical depth at 1051 nm and single scattering albedo are shown. The Inter Tropical Convergence Zone locations are indicated based on observations such as cloudiness, change in wind direction, etc.

ship) prevailed during this period was bringing the ship exhaust plume to the stem, whenever the ship speed was low or it stopped for other experiments. This affected both the aerosol and air chemistry experiments. The data are screened for the ship exhaust contamination, taking into account the wind speed and direction as described in a later section. The third transect was from 20°S to 15°N in the south to north direction, in the 58° to 63°E longitude region. In this return leg, data could be collected both at the south and north of the ITCZ. The wind direction which was predominantly from the southeast direction during the first half of the transect changed to northwest direction around the equator which brought the polluted continent air. The fourth transect was entirely in the Arabian Sea, along 15°N, between 60° and 72°E longitude, in the west to east direction, towards India. The fifth and the last transect, made during 7 to 10 March was parallel to the Indian Coast in the northwest direction. The last leg of this transect included coordinated measurements with NOAA's research vessel *Ronald H. Brown* (*Ron. Brown*). Both the ships sailed together, towards the northwest direction from 15.8°N, 69.8°E to 17.4°N, 68.4°E, from 9 March 12 UTC to 10 March 11 UTC, for about one diurnal cycle. During this transect the wind was predominantly from the northeast direction, and the ships were positioned such that the ship exhaust from one ship did not contaminate the other.

## Experiments

Measurements of the aerosol optical properties, downward solar radiation flux at the surface, concentrations of trace gases, meteorological and oceanic parameters were made onboard *Sagar Kanya* along the cruise track. Table 1 gives the list of measurements and the instruments used, the results of which are presented and discussed in the present work.

The columnar aerosol optical depth was measured using a hand-held sun-photometer. Measurements were

**Table 1.** Aerosol and radiation-related measurements carried onboard *Sagar Kanya* the results of which are presented and discussed in this work

Parameter measured	Instrument used	Responsibility
<i>Aerosols</i>		
Optical depth at 399, 497, 667, 848 and 1051 nm	Hand-held sunphotometer	Physical Research Laboratory, Ahmedabad
Optical depth at 1020 nm	Microtops photometer	-do-
Aerosol size distribution	Quartz crystal microbalance	-do-
Scattering coefficient ( $1 \text{ km}^{-1}$ )	Nephelometer	C4/Center for Atmospheric Sciences, Scripps Institution of Oceanography, UCSD, La Jolla
Absorption coefficient ( $1 \text{ km}^{-1}$ )	Particle soot absorption photometer	-do-
<i>Radiation</i>		
Direct solar radiation intensity ( $\text{W/m}^2$ ) – total and near IR	Hand-held pyrheliometer	Physical Research Laboratory, Ahmedabad
Global radiation flux ( $\text{W/m}^2$ ) – total and near IR	Gimbals mounted pyranometer	C4/Center for Atmospheric Sciences, Scripps Institution of Oceanography, UCSD, La Jolla

made at five spectral bands with center wavelengths at 399, 497, 667, 848 and 1051 nm and bandwidths (full width at half maximum) 19, 13, 14, 14 and 25 nm respectively. No data were collected if the Sun was obscured by clouds or if clouds were present (about  $\pm 30^\circ$ ) around the vicinity of the Sun. The instrument was equipped with a 'sample and hold' facility to register the maximum voltage value when pointed towards the Sun, thus eliminating any operator bias in the measurement. The same instrument was used in the earlier three INDOEX cruises made in 1996, 1997 and 1998. The instrument was calibrated regularly before and after each cruise at the hill station, Mount Abu. More information on aerosol optical depth determination can be obtained from Jayaraman *et al.*<sup>4</sup>. A 'microtops' sun-photometer was also employed to measure the columnar water vapour and ozone concentrations and aerosol optical depth at 1020 nm. The water vapour and ozone results will not be discussed here. Both the sun-photometer observation and the microtops observation were made from the ship bridge, which facilitated an unobstructed view of the Sun.

Apart from the columnar optical depth measurements, aerosols found within the marine boundary layer were studied for their size distribution and optical properties by sampling the air at frequent intervals. A quartz crystal microbalance (QCM) cascade impactor system was used to measure the aerosol mass concentration ( $\mu\text{g}/\text{m}^3$ ) in ten different size bins, with 50% efficiency cut-off radii at 12.5, 6.4, 3.2, 1.6, 0.8, 0.4, 0.2, 0.1, 0.05 and 0.025  $\mu\text{m}$ . The air sample was drawn through the impactor at a rate of 0.24 l/min. A pair of quartz crystal wafers was employed in each stage of the impactor and the relative frequency change was measured to obtain the accumulated aerosol mass. The time duration of each measurement varied from 10 to 20 min depending on the aerosol loading of the atmosphere. A total of about eight measurements were made each day. The mass values were converted into number density by taking the appropriate radii for each stage and the density of single aerosol particle as 2 g/cc. In the absence of quoted accuracy from the manufacturer, we estimate the overall maximum uncertainty in the derived mass concentration values, as 25% for all the 10 stages.

The aerosol scattering coefficient was measured in real time using a nephelometer. The instrument uses in-built flashlamp and detector to measure the scattered light. In the present set up, the sample air was drawn at a rate of 10 l/min and the scattering coefficient was measured at 530 nm. Pressure and temperature of the scattering air volume were monitored online and the values were used to compute the Rayleigh scattering coefficient. From the measured total scattering coefficient the Rayleigh contribution was subtracted and the resultant aerosol scattering coefficient values were averaged for every 5 min interval and stored. The instrument was calibrated everyday using clean air for about 15 min and checked for any drift in the

flash lamp, detector characteristics. The scattering coefficient data measured by the nephelometer were accurate to within  $\pm 7\%$  based on laboratory closure experiments<sup>5</sup>.

A particle/soot absorption photometer (PSAP) was used to measure the absorption coefficient of the aerosols in real time along with the scattering coefficient. The operation principle is based on the measurement of the change in the optical transmission of a paper filter caused by particle deposition. The change in transmission is related to the absorption through Beer's law. The absorption coefficient is calculated using a calibration transfer coefficient specific to the instrument. The wavelength of operation was 565 nm (factory set). The airflow through the instrument was fixed at a rate of 2 l/min and was continuously monitored and controlled. The filter papers were continuously changed, twice a day in the polluted region and once a day elsewhere. The main source of error in PSAP measurements is the accurate estimate of the spot area on the filter paper and the flow rate<sup>6</sup>. Another source of uncertainty is the possibility of radiation loss by scattering of light by the aerosols impacted on the filter sample. Taking all the possible uncertainties into account, Bond *et al.*<sup>6</sup> estimated an overall maximum error of  $\pm 20\%$  for the absorption data from PSAP. The QCM, Nephelometer and PSAP were made to draw air sample from the same air inlet tube, which was a vertical hose pipe mounted along the right side (starboard side) of the ship. The air intake was at a height of about 12 m from the sea surface.

## Results and discussions

### Aerosol optical depth

Figure 2 shows the plot of the aerosol optical depth values measured at the five wavelengths as a function of latitude.

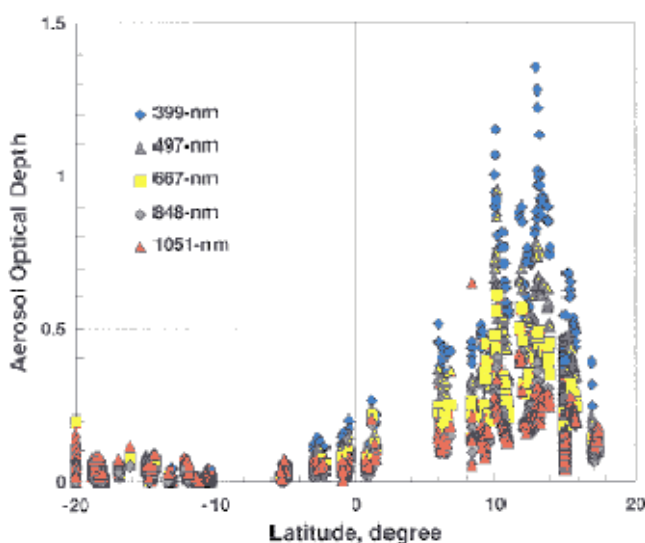


**Figure 2.** Aerosol optical depths, measured along the cruise track, are plotted as a function of latitude to show the large north-south asymmetry seen in the values. The latitude gradient persists from north down to about  $5^\circ\text{S}$ , where the ITCZ was located.

Low values are obtained, in the range of 0.1 and less, at all the wavelengths, south of the ITCZ. However in the north,  $d_l$  increases and the increase is steeper as one enters more into the Arabian Sea. Stronger latitude gradient is seen for the lower wavelength region than compared to the higher wavelengths. As sub-micron size particles (radii less than  $1\ \mu\text{m}$ ) are known to contribute strongly to the lower wavelength optical depth, the sharp increase seen in  $d_l$  at lower wavelength indicates an increase in the concentration of the sub-micron particles over the Arabian Sea. Similarly, coarse particles of size greater than about  $1\ \mu\text{m}$  are found to influence  $d_l$  at higher wavelengths (e.g. at 1051 nm in the present work). These particles are mainly wind-derived soil dust<sup>7</sup> or sea salt particles, produced while the entrained air bubbles burst at the surface of the sea water<sup>8</sup>. While soil dust is mainly confined around the vicinity of the arid and semi-arid regions of the continents, and have limited range over the ocean surface, the sea salt particles are the dominant contributor to the coarse mode of the aerosol size distribution in the remote marine atmosphere<sup>9</sup>.

Figure 3 shows the comparison between the aerosol optical depth measured by the Microtops at 1020 nm and the sun-photometer measured values at 1051 nm. The results of the statistical fit are shown in the plot. The negative intercept indicate that, on an average, the 1051 nm optical depth is less than the 1020 nm value by a value of about 0.031. This could be due to the fact that  $d_l$  in general decreases with  $l$ . However there were occasions, when the 1051 nm optical depth was found higher than that of the 1021 values. Also there is a considerable spread in the

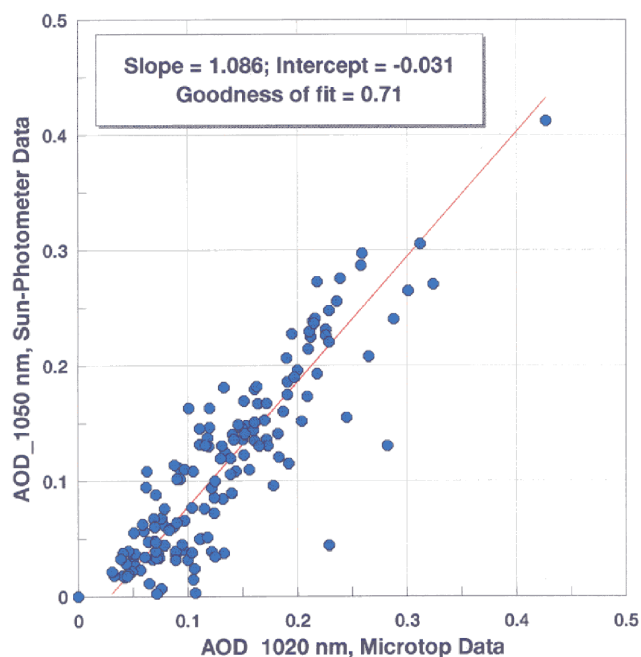


**Figure 3.** Aerosol optical depth data measured at 1051 nm using PRL's sun-photometer are compared with the Microtops sun-photometer data for 1020 nm. Results of the statistical fit are shown in the top left corner.

data as indicated by a correlation coefficient of 0.71. The negative intercept and the spread in the scatter plot could also mean an inherent offset (by a value of 0.031 in  $d_l$ ) in one of the instruments with respect to other. The other reason for the observed spread in the data could be the finite time difference between the sun-photometer and microtops measurements, which was typically 5 to 10 min, as both the instruments were operated manually. As the higher wavelength optical depths are influenced by the coarse mode sea salt particles, the possibility of change in their concentration due to changing wind speeds cannot be ruled out.

The aerosol optical depth spectrum can be fitted by a power law of the type

$$d_l = bl^{-a}, \quad (1)$$

where  $l$  is expressed in  $\mu\text{m}$ . The wavelength exponent  $a$  describes the spectral behaviour of the optical depth and the coefficient,  $b$  is the measure of the vertical column burden of aerosols and is equal to  $d$  at  $l = 1\ \mu\text{m}$ . The advantage of this relationship is that  $d$  can be estimated for unknown  $l$ s from a known set of  $d$  and  $l$  values. However, we find that there can be large errors in the estimated optical depths for wavelength greater than  $1\ \mu\text{m}$ , if coarse mode particles, of radius greater than  $1\ \mu\text{m}$ , are present dominantly in the aerosol size distribution. Examples of such deviations are seen on several occasions in our measurements. Figure 4 shows two such examples, where one set of measurement was made on 24 January, close to the coast of Thiruvananthapuram and the other was made on 9 March, more north in the Arabian Sea (see Figure 1 for the locations). The fitted Angstrom curve is found to explain all the data points except the 1050 nm data points. The actual data points are higher (by 23% for the 24 January and by 35% for the 9 March cases) than the predicted values by the Angstrom curve. Note that the optical depths are corrected for water vapour absorption, which contribute less than 0.02 to the total optical depth at 1050 nm. The columnar integrated water vapour content measured independently using microtops showed a value of 2.2 cm over the coast of Thiruvananthapuram on 24 January and 2.1 cm over the interior Arabian Sea on 9 March. Similar observations of higher optical depth at larger wavelengths were reported earlier<sup>10</sup>. Increase in aerosol optical depth at wavelengths greater than 1000 nm, caused by coarse particles, has serious implications in climate modeling and remote sensing applications. In the absence of aerosol optical depth above 1000 nm it is customary to extrapolate the Angstrom curve and estimate optical depth values for higher wavelengths. This can underestimate the optical depth by a few tens of per cent if coarse aerosols are present as it has been seen in the case of Arabian Sea. It is also applicable for the open ocean region, where wind speeds greater than about 10 m/s are known<sup>11</sup> to produce large amount of coarse sea salt particles. Excluding the

1051 nm data, Angstrom curve was fitted for all lower wavelength data collected during the cruise. Over the Arabian Sea the  $a$  values are in the range of 1.3 to 1.7 while over the pristine Indian Ocean region the values are low and are in the range of 0.5 to 0.7. These values are similar to our earlier findings<sup>4</sup> made during the pre-INDOEX cruise in 1996. The only other data available for the Indian Ocean region prior to this was by Tomasi and Prodi<sup>12</sup> who obtained an  $a$  value of 0.6, northeast of the Seychelles islands in January–February 1979 which compares well with our present pristine Indian Ocean value.

The 1999 aerosol optical depth values are found to be higher than all the earlier values obtained during 1996, 1997 and 1998 over the Arabian Sea and the coastal region. An annual variation is seen in the data set, with 1996 and 1998 recording low values and the following years 1997 and 1999 showing high optical depth values. Large variations are seen in the optical depth at lower

wavelengths than compared to at higher wavelengths. Figure 5 shows 399 nm  $d_l$  values measured during the 1998 and 1999 periods. For comparison the 1051 nm values are also shown. More than a factor of two increase is seen in the lower wavelength optical depth presumably caused by the anthropogenically produced sub-micron particles brought from the continents. As it is known, 1998 was an *El Nino* year and 1999 was more a *La Nina* year. A stronger inversion and larger number of anti-cyclones observed during the early 1999 had resulted in trapping the pollutants in the surface layer, which were transported to the ocean region and got accumulated. During 1998 the inversion was weaker over India which resulted in pollutants raising higher, where a sizable portion got caught in the westerlies and moved east with a proportionate reduction in the amount of pollutants reaching the Indian Ocean (T. N. Krishnamurti, Florida State University, private commun.). Thus the 1999 data, presented in this work are an example of the extreme case scenario useful for comparison with model results and with any future measurements over these regions.

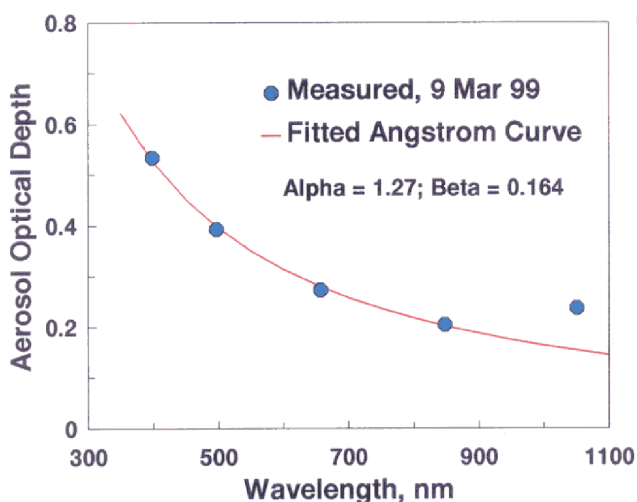
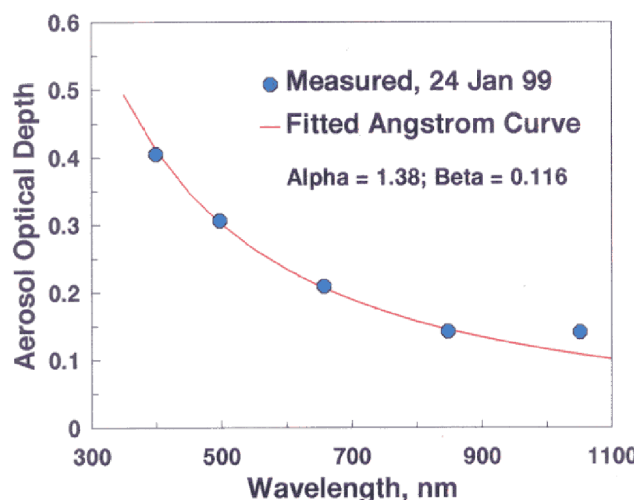


**Figure 4.** Examples of the measured aerosol optical depth values, curve fitted using eq. (1). The optical depth at 1050 nm is seen falling outside the fitted curve on several occasions during the cruise.

### Aerosol size distribution

The QCM data on the aerosol mass concentration and size distribution have been used further to interpret the observed aerosol optical depth spectrum. Figure 6 shows the measured aerosol mass concentration values along the cruise track as a function of day number. Day number 20 corresponds to 20 January and 70 corresponds to 11 March, which is the end date of the cruise. The mass concentrations measured individually at 10 different size bins are grouped into three categories, viz. coarse mode, accumulation mode and nucleation mode. The coarse mode contains particles of radii between 1 and 10  $\mu\text{m}$

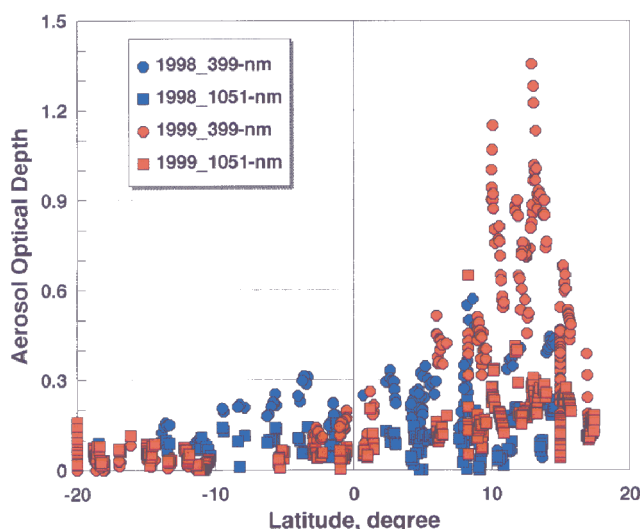


**Figure 5.** Comparison between the 1998 and 1999 aerosol optical depth values. Optical depth at lower wavelengths during the 1999 observations was found to be much higher than that of the 1998 values.



(sum of channels 2, 3 and 4 of the QCM), the accumulation mode contains particles in the radii range 0.1 to 1  $\mu\text{m}$  (sum of channels 5, 6, 7 and 8) and the nucleation mode corresponds to particles of radii less than 0.1  $\mu\text{m}$  (sum of channel 9 and 10). Data correspond to channel 1, which collects all aerosols greater than 12.5  $\mu\text{m}$  is not included in the present analysis. One of the important features seen in the aerosol mass concentration data (Figure 6, bottom panel) is that the nucleation mode aerosols are systematically higher over the Arabian Sea, with values ranging from 20 to 50  $\mu\text{g}/\text{m}^3$  than compared to over the Indian Ocean, south of the ITCZ, where the values are around 10  $\mu\text{g}/\text{m}^3$ . The nucleation mode aerosols undergo condensation growth and coagulate with other particles to grow as the accumulation mode particles. As the precursors for the formation of the nucleation mode particles mostly come from the continents<sup>13</sup>, the newly formed particles are found in abundance near the coastal region. Compared to nucleation mode aerosols, accumulation mode aerosols are relatively long lived, and are found dispersed over a longer distance (Figure 6, middle panel). Mass concentration in the range of 50  $\mu\text{g}/\text{m}^3$  and above are seen for the accumulation mode particles near the Indian coast and the values are less than 50  $\mu\text{g}/\text{m}^3$  and lower at the south of the ITCZ. One of the important observations is that in the return leg of the cruise (day numbers above 58) over the Arabian Sea, towards north, the accumulation mode particles concentration is low, while the nucleation mode shows consistently very high values. This support our earlier hypothesis that as the wind blows from the continent (in the present case, India) it carries with it the precursor gases such as sulfur dioxide, which get converted and nucleated along its trajectory into small particles of size less than 0.1  $\mu\text{m}$ . However, along the down wind the particles grow, and the concentration of the accumulation mode particles increases as it has been seen along the south coast of India in the forward leg data. The coarse mode particles (Figure 6, top panel) seen over the marine atmosphere are mainly sea-spray particles with occasional intrusion of wind blown mineral dust particles from the surrounding continents.

The coarse particle mode is better seen in the aerosol number density distribution curve (Figure 7) calculated from the mass concentration data, assuming an uniform density of 2 g/cc for particles in all the size ranges. Few examples of daily average values are only shown to highlight the important differences seen in the aerosol size distribution at different regions. The differences are mainly seen in the nucleation mode (radii less than 0.1  $\mu\text{m}$ ) and in the coarse mode (radii greater than 1  $\mu\text{m}$ ) size regions. The 24 January and 9 March data show clearly an increase in the concentration of the coarse mode particles. As discussed earlier, these particles are responsible for the increase in aerosol optical depth at higher wavelengths, at 1000 nm and above. The 11 February and 25 February data correspond to the pristine

region, south of the ITCZ and far away from the Indian coast. The main difference is that the concentration of the nucleation mode particle is less compared to that at the north of the ITCZ. This has resulted in the low aerosol optical depth observed at the 399 nm in the pristine

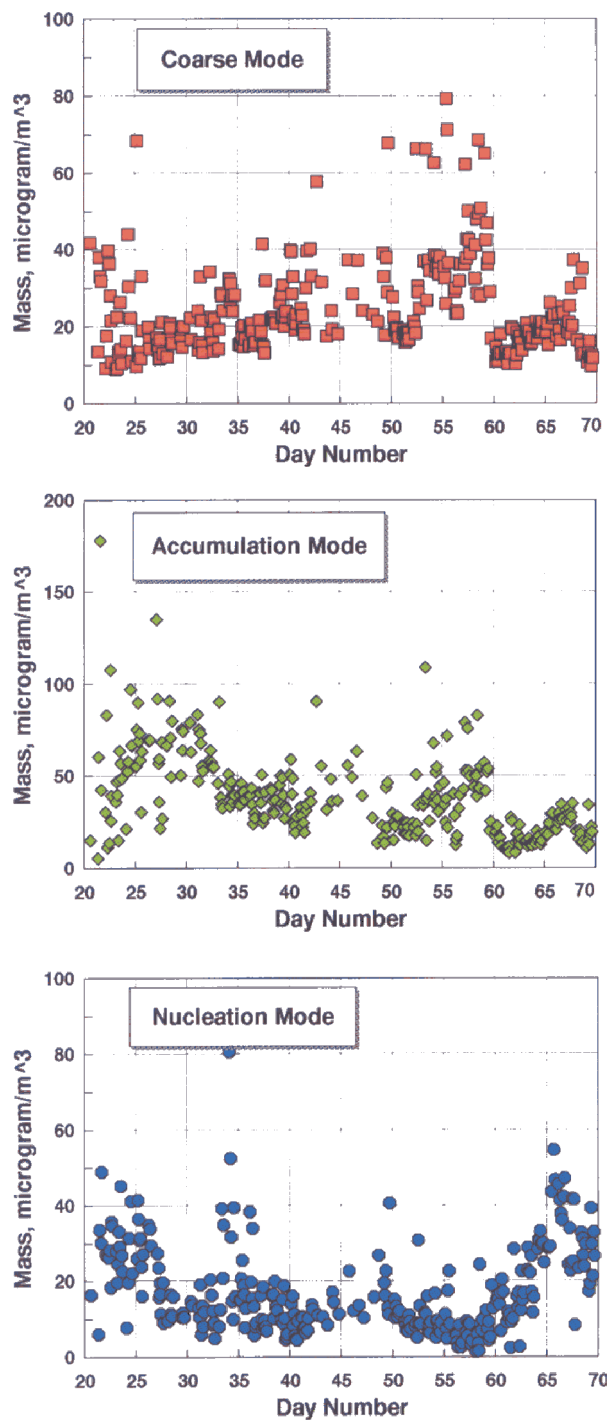


**Figure 6.** Aerosol mass concentration measured using the quartz crystal microbalance. Individual mass data from each stage is summed according to coarse mode (sum of channel 2, 3 and 4, corresponding to radius 1 to 10  $\mu\text{m}$ ), accumulation mode (sum of channel 5, 6, 7 and 8, corresponding to radius 0.1 to 1  $\mu\text{m}$ ) and nucleation mode (sum of channel 9 and 10, corresponding to radius less than 0.1  $\mu\text{m}$ ).

region. For example, the measured aerosol optical depth is in the range of 0.06 to 0.08 for 399 nm on 25 February whereas the corresponding values are in the range of 0.4 to 0.6 on 24 January and 9 March. Thus the aerosol optical depth spectrum is mainly determined by the aerosol size distribution. The nucleation mode particles, produced mainly from gas to particle conversion, are responsible for the increased aerosol optical depth seen at lower wavelengths (less than 500 nm), whereas the aerosol optical depths at higher wavelengths (greater than 1000 nm) are mainly determined by the presence of the mechanically produced coarse particles.

**Aerosol scattering and absorption,  $s_s$  and  $s_a$**

The aerosol scattering and absorption coefficients were measured continuously throughout the cruise, using nephelometer and PSAP. The data were averaged and stored at every 5 min interval in the case of nephelometer and at every minute in the case of PSAP. All the data are screened carefully for the local contamination, particularly from the ship exhausts. Wind direction and speed, measured using an anemometer fitted near to the inlet tube, are used as the main criteria to screen the obtained data. As the air inlet tube was mounted at the starboard

side of the ship, data corresponding to wind direction 0 to 90 degree with respect to ship head are only used for analysis. Also, to avoid the possibility of small eddies generated around the ship bringing the ship pollutants to the sample inlet, data corresponding to only wind speed greater than or equal to 3 m/s are considered. Further when the ship was berthed at Port Luis, Mauritius from 11 to 17 February, the data were found contaminated by several local sources around the port and hence not used in the analysis. Figure 8 shows the results of the obtained scattering and absorption coefficient ( $1 \text{ km}^{-1}$ ) values, which are plotted as a function of the day number. From day number 31 to 55 the ship was at the south of the ITCZ, sampling mainly the pristine air. However, during this period, most of the occasions, the wind was from the south, southeast directions, and for the ship sailing towards west, it was from the stern (outside the 0 to 90° corridor) and hence the data are screened out. Of the 18 cruise days within the pristine region, we could collect

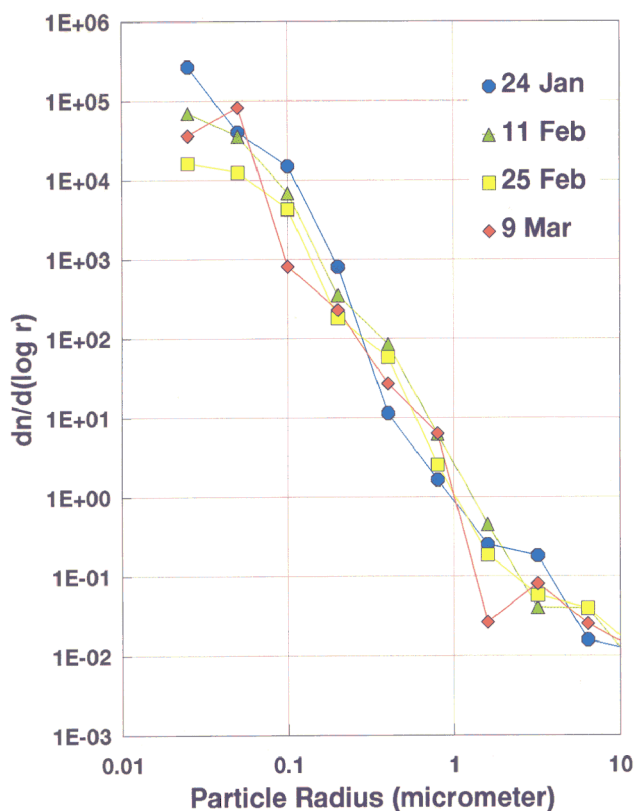


**Figure 7.** Aerosol size distribution obtained from the mass concentration data for few selected days. Day-to-day and regional differences are seen mostly in the size ranges less than 0.1  $\mu\text{m}$  and greater than 1.0  $\mu\text{m}$  radius.

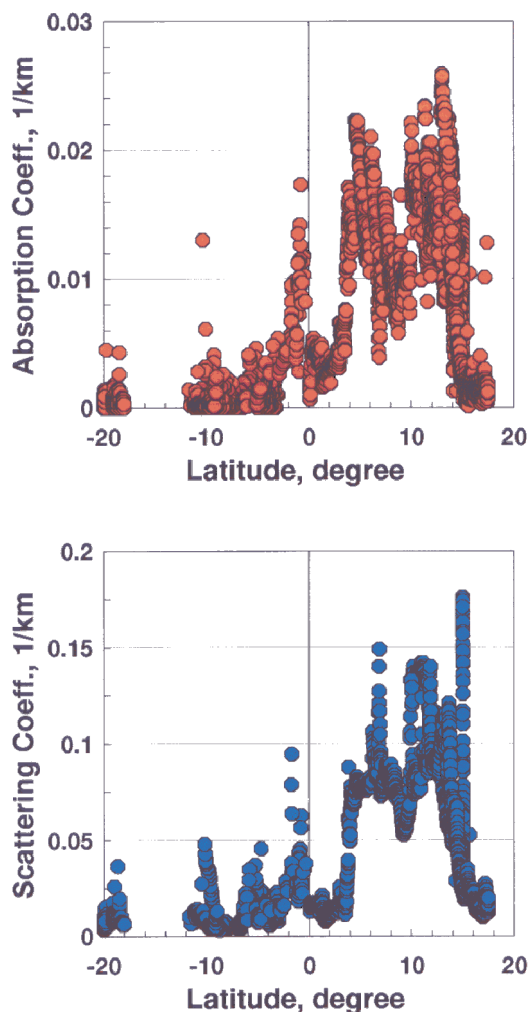


**Figure 8.** Latitude variation seen in aerosol absorption (top) and scattering (bottom) coefficients along the cruise track. The data are screened for possible contamination from the ship's exhaust. The intermittent data gaps are caused due to the screening process.

uncontaminated data only on days 40, 41, 49, 52, 53 and 54. In the north of ITCZ, uncontaminated data could be obtained for 19 days.

Compared to aerosol optical depth measurement, which is a total columnar measurement, the nephelometer and PSAP data on aerosol scattering and absorption coefficients are for the aerosols present within the marine boundary layer (MBL). Nevertheless, the overall features of high north-south gradient seen in both the data sets confirm that the boundary layer aerosols have the major contribution to the observed columnar optical depth. A scattering coefficient value of  $0.025 \text{ km}^{-1}$  or less is considered to be a 'low' value, between  $0.025$  and  $0.05 \text{ km}^{-1}$  represent 'medium' aerosol loading and values above  $0.05 \text{ km}^{-1}$  represent a 'high' aerosol concentration. In the present data, a sharp increase is seen in the scattering (and in absorption) which changes from a low value of less than  $0.015 \text{ km}^{-1}$  to a high value of greater than  $0.05 \text{ km}^{-1}$  as the ship enters the northern hemisphere around day 55. The scattering and absorption values continue to increase till about  $5^\circ\text{N}$ , but started decreasing when the ship sailed in the northwest direction away from India. A minimum scattering value of  $0.04 \text{ km}^{-1}$  was obtained in the Arabian Sea when the ship was at the farthest point from the coast of India on day 61. As the ship started sailing towards the India coast from day 61 onwards, both the scattering and absorption increase again and reach the highest value (more than  $0.1 \text{ km}^{-1}$  for scattering and more than  $0.02 \text{ km}^{-1}$  for absorption) on days 65 and 66 when the ship was close to the Indian coast.

In Figure 9, aerosol scattering coefficient and the mass concentration obtained over the Arabian Sea are plotted together to bring out the similarity seen between the two data sets. Though the overall spatial variation features compare, there are discrepancies between the QCM and nephelometer data caused presumably due to the change in the humidity of the sampling air. The scattering measurement responds instantaneously to change in particle size if the relative humidity changes. In the case of mass concentration measurement, the particles are allowed to settle on the quartz wafer and the integrated mass change is measured typically after 20 min. This may lead to evaporation loss of the adsorbed water from the particles, aggregated by the low pressure in the impactor stages. The humidity effect could be more severe if the relative humidity values are more than 80% (ref. 14). For the data period shown in Figure 9, the ambient humidity was in the range of 70 to 80%, and at few occasions found to exceed 80% and lie in the 80 to 90% range. Correlating the aerosol mass with the simultaneously measured scattering coefficient, for the Arabian Sea region we get a scattering to mass concentration ratio of  $2.27 \text{ m}^2/\text{g}$ . This is within the range of 1.4 to  $5.0 \text{ m}^2/\text{g}$  as reported by Charlson *et al.*<sup>15</sup>. Waggoner *et al.*<sup>16</sup> obtained a mass to scattering value of  $3.3 \text{ m}^2/\text{g}$  for continental aerosol and Hoppel *et al.*<sup>17</sup> obtained a value of  $1.67 \text{ m}^2/\text{g}$  for the marine aerosols, along the east coast of

the United States. The present value obtained for the Arabian Sea is typically between the marine and the continental values as reported in the above referred works.

### Single scattering albedo, $w$

A combination of the scattering and absorption measurements is useful in estimating the single scattering albedo for aerosols, which is defined as the ratio of the scattering to the total extinction (scattering + absorption).

$$w = S_s / (S_s + S_a). \quad (2)$$

Though the scattering was measured at 530 nm and the absorption at 565 nm, we assume that the variation of scattering and/or absorption is small within these two wavelengths interval. Figure 10 shows the  $w$  values calculated from the scattering and absorption data. Daily mean values of  $S_s$  and  $S_a$  are calculated and used in deriving the  $w$  values. The vertical bar shows one standard deviation of the mean. As pointed out earlier, both the scattering and absorption data have uncertainty in the range of  $\pm 7\%$  and  $\pm 20\%$  respectively. Proportionately there is a corresponding uncertainty in the computed  $w$  values. In the expression for  $w$ , since scattering appears in both numerator and denominator, and the value of the absorption is much less

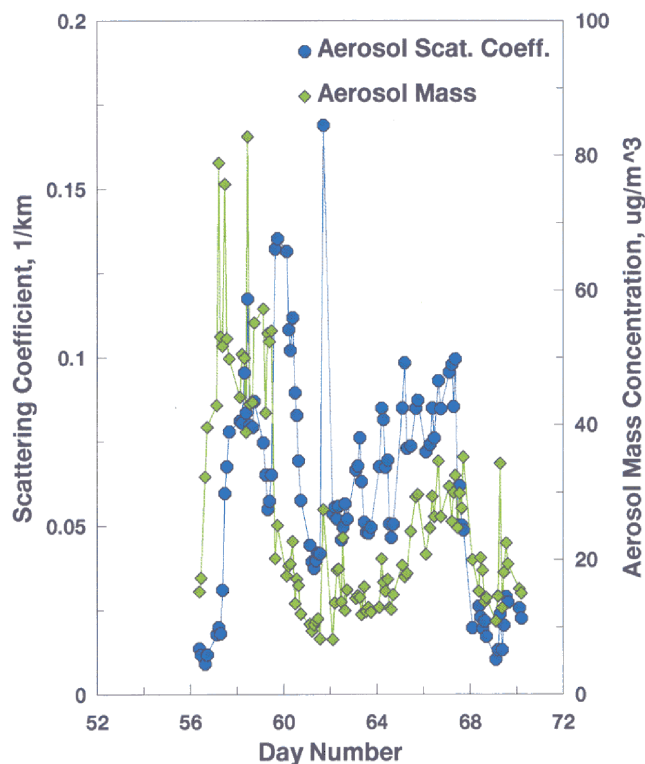


**Figure 9.** Comparison of aerosol mass concentration (accumulation mode) and scattering coefficient obtained over the Arabian Sea and the coastal region. The ratio of aerosol scattering coefficient to aerosol mass is found to be  $2.27 \text{ m}^2/\text{g}$ .



than the scattering, the computed uncertainty for  $w$  is less than the individual uncertainty values for the scattering and absorption. For the present data, the computed uncertainty values are less than  $\pm 2.5\%$  for  $w > 0.9$  and between  $\pm 2.5\%$  and  $\pm 5\%$  for  $0.8 < w < 0.9$ .

The  $w$  values are in the range of 0.8 to 0.9 for aerosols present over the Arabian Sea and the coastal India, compared to a value of 0.95 and more for the open ocean region, south of the ITCZ. Low  $w$  values are found more close to the coastal region, where the measured columnar aerosol optical depth values (at 497 nm) showed high values. For a  $w$  value of 0.8, and optical depth in the range 0.4 to 0.7 (values found near the coast) the columnar optical depth due to aerosol absorption amounts to 0.08–0.14. This obtained columnar aerosol absorption value is much higher than the combined absorption by all known molecular gases in this spectral region. Carbonaceous aerosols (soot particles) from fossil fuel and biomass burning could be one of the main contributors to the aerosol absorption.

The columnar aerosol absorption could be even higher if we consider the fact that aerosol single scattering albedo can decrease with altitude. This is because, as relative humidity decreases with altitude, the hygroscopic aerosols, like sea salt (which is non-absorbing) shrink in size and contribute less to the total optical depth than compared to at the surface. Also, the major absorbers like soot are smaller in size and distributed uniformly upwards to greater

extents compared to the sea salt aerosols which are generally larger in size. Even if we take the surface single scattering albedo constant with altitude, the value of extinction coefficient (scattering + absorption) at the surface of about 0.08 to 0.16 (Figure 8) and column value of optical depth of about 0.4 to 0.8 translates to an aerosol scale height of about 5 km which is very high. In other words, the above finding suggests that absorbing aerosol layers are present even above the marine boundary layer, if the aerosols are not uniformly mixed. This is also supported by the C-130 aircraft profiles of aerosol scattering and absorption coefficients obtained over the Arabian Sea (J. Ogren, NOAA, unpublished data).

### Summary

As part of the INDOEX-IFP study, characteristics of aerosols found over the Arabian Sea and the Indian Ocean were studied using data collected during the ORV *Sagar Kanya* cruise from 20 January to 12 March 1999. Both the aerosol optical properties and mass concentration show large latitudinal differences particularly between north and south of the ITCZ (which was located between  $0^\circ$  and  $5^\circ\text{S}$ ). For example, the aerosol optical depth values were less than 0.1 south of the ITCZ but increased by a factor of 4 or more north of the ITCZ. The gradient could be due to both the dilution of the plume by advective dispersal and due to the removal of particles from the air mass as it moves from the continent to the interior ocean region. The major known scavenging processes are, coagulation of smaller particles to form bigger particles, gravitational settling of bigger particles, and rain wash. One of the important differences between the land and the ocean regions is that, particles once settled on the sea are irrecoverably lost whereas particles settled on the land can be airlifted again depending on the prevailing surface wind conditions. The observed latitude gradient in the optical depth is deeper for visible and smaller wavelengths, implying the role of submicron size particles in controlling the aerosol optical depth spectrum. From a series of optical and chemical observations made from Kaashidhoo Climate Observatory (established in a tiny island at  $5^\circ\text{N}$  and  $73.5^\circ\text{E}$ , in Maldives), Satheesh *et al.*<sup>18</sup> have found that the submicron particles are mainly composed of soot, sulfate, ammonium and organics, and of these about 65% are of anthropogenic origin. The steep increase seen in the optical depth values at lower wavelengths, as one moves towards the coastal region is believed to be caused due to the increase in the concentration of these particles.

The role of aerosol size distribution in controlling the aerosol optical depth is studied. It is known that  $d_l$  at lower wavelengths (less than 500 nm) are influenced by the amount of submicron particles, whereas  $d_l$  at higher wavelengths (greater than 1000 nm) are influenced by the presence of the mechanically produced coarse particles. In the

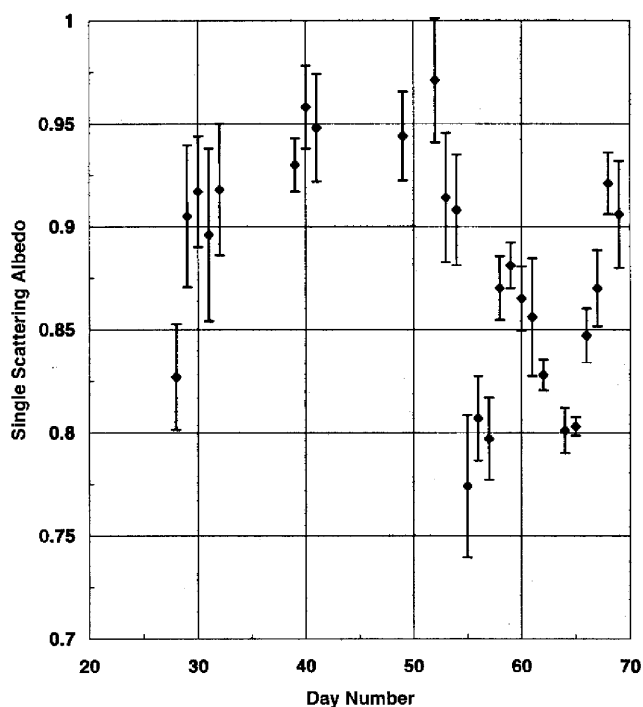


**Figure 10.** Single scattering albedo  $w$ , obtained from the daily averaged aerosol scattering and absorption data. Vertical bar shows one standard deviation of the mean. The uncertainty in the computed  $w$  values is less than  $\pm 2.5\%$  for  $w > 0.9$  and between  $\pm 2.5\%$  and  $\pm 5\%$  for  $0.8 < w < 0.9$ .

marine boundary layer, the coarse particles are mainly sea salt aerosols and their amount depends on the surface wind speed and sea-state. We show that fitting the aerosol optical depth spectrum using a single wavelength exponent curve can become erroneous, if coarse mode particles of radius greater than  $1\ \mu\text{m}$  are present dominantly in the aerosol size distribution. In other words, estimation of  $d_l$  values at  $l > 1\ \mu\text{m}$ , using the wavelength exponent  $a$  derived mainly from  $d_l$  values obtained at lower wavelengths, can lead to erroneous results.

Aerosol mass concentration data reveal that the nucleation mode aerosols (radius  $< 0.1\ \mu\text{m}$ ) are systematically higher over the Arabian Sea, with values ranging from 20 to  $50\ \mu\text{g}/\text{m}^3$  than compared to over the Indian Ocean, south of the ITCZ, where the values are around  $10\ \mu\text{g}/\text{m}^3$ . A reduction observed in the concentration of nucleation particles, with increasing distance from the coast, and an increase in the accumulation mode particles (radius  $< 0.1\ \mu\text{m}$ ) concentration suggests the growth of nucleation mode particles. The accumulation mode aerosols are relatively long lived, and a mass concentration, in the range of  $50\ \mu\text{g}/\text{m}^3$  and above are seen north of the ITCZ and lower values towards the south. Correlating the aerosol mass with the scattering coefficient, in the Arabian Sea region, we get a scattering to mass concentration ratio of  $2.27\ \text{m}^2/\text{g}$ , which is between the values reported for the continental and marine aerosols by other workers<sup>15-17</sup>. The single scattering albedo,  $w$  derived from the scattering and absorption data, for the aerosols present over the Arabian Sea is around 0.9 while for aerosols present near the Indian coast,  $w$  can be as low as 0.8. Low  $w$  associated with high optical depth measured near the Indian coast implies large absorption of radiation by particles. Comparison of the surface measured extinction coefficient with the columnar optical depth shows that the absorbing aerosol layers can extend even above the marine boundary layer. The columnar aerosol absorption found at the coastal region for the visible wavelength is much higher than the combined absorption by all known molecular gases. This additional absorption by aerosols could be responsible for the high aerosol radiative forcing

observed at the surface during earlier occasions<sup>4,18,19</sup> over this region.

1. Charlson, R. J., Langner, J., Rohde, H., Leovy, C. B. and Warren, S. G., *Tellus*, 1991, **43AB**, 152–163.
2. Hansen, J., Sato, M. and Ruedy, R., *J. Geophys. Res.*, 1997, **102**, 6831–6864.
3. Ramanathan, V. *et al.*, Indian Ocean Experiment: A multi-agency proposal for field experiment in the Indian Ocean, C4 pub 162, Scripps Institution of Oceanography, La Jolla, California, 1996, pp. 83.
4. Jayaraman, A., Lubin, D., Ramachandran, S., Ramanathan, V., Woodbridge, E., Collins, W. D. and Zalpuri, K. S., *J. Geophys. Res.*, 1998, **103**, 13827–13836.
5. Anderson, T. L. and Ogren, J. A., *Aerosol Sci. Technol.*, 1998, **29**, 57–69.
6. Bond, T. C., Anderson, T. L. and Campbell, D., *Aerosol Sci. Technol.*, 1999, **30**, 582–600.
7. Tegan, I. and Lacis, A. A., *J. Geophys. Res.*, 1996, **101**, 19237–19244.
8. Exton, H. J., Latham, J., Park, P. M., Perry, S. J., Smith, M. H. and Allan, R. R., *Quart. J. R. Meteorol. Soc.*, 1985, **111**, 817–837.
9. Prospero, J. M., *J. Geophys. Res.*, 1979, **84**, 725–731.
10. Krishna Moorthy, K., Satheesh, S. K. and Krishna Murthy, B. V., *J. Atmos. Solar Terr. Phys.*, 1998, **60**, 981–992.
11. Hoppel, W. A., Frick, G. M., Fitzgerald, J. W. and Larson, R. E., *J. Geophys. Res.*, 1994, **99**, 14433–14459.
12. Tomasi, C. and Prodi, F., *J. Geophys. Res.*, 1982, **87**, 1279–1286.
13. Quinn, P. K., Kapustin, V. N., Bates, T. S. and Covert, D. S., *J. Geophys. Res.*, 1996, **101**, 6931–6951.
14. Hegg, D., Larson, T. and Yuen, P. F., *J. Geophys. Res.*, 1993, **98**, 18435–18439.
15. Charlson, R. J., Ahlquist, N. C. and Horvath, H., *Atmos. Environ.*, 1968, **2**, 455–464.
16. Waggoner, A. P., Weiss, R. E., Ahlquist, N. C., Covert, D. S., Will, S. and Charlson, R. J., *Atmos. Environ.*, 1981, **15**, 1891–1909.
17. Hoppel, W. A., Fitzgerald, J. W., Frick, G. M., Larson, R. E. and Mack, E. J., *J. Geophys. Res.*, 1990, **95**, 3659–3686.
18. Satheesh, S. K. *et al.*, *J. Geophys. Res.*, 1999, **104**, 27421–27440.
19. Jayaraman, A., *Curr. Sci.*, 1999, **76**, 924–930.

ACKNOWLEDGEMENTS. We thank the chief scientist of the cruise and the crew members for the assistance provided for the deployment of the instruments in the ship. The ship, ORV *Sagar Kanya* was provided by the Department of Ocean Development, Govt India. The Indian experiments were funded by the Department of Space, Govt India and the Council of Scientific and Industrial Research, India through the INDOEX-India project office. The US experiments were funded through the NSF grant to C4.